

# THE SARAF-LINAC BEAM DYNAMICS

N. Pichoff, B. Dalena, D. Uriot, CEA/IRFU, Gif-sur-Yvette, France

## Abstract

SNRC and CEA collaborate to the upgrade of the SARAF Accelerator to 5 mA CW 40 MeV deuteron and proton beams (Phase 2). This paper presents the beam dynamics in the reference design of the SARAF-LINAC, from the 4 m long 176 MHz RFQ to the HWR Superconducting linac's end. The beam losses, mostly in longitudinal direction, estimated from error studies, are compared with acceptable losses defined for hands-on maintenance.

## INTRODUCTION

Israeli's SNRC solicited CEA (France) to contribute to the development of phase 2 of the SARAF accelerator [1].

In order to deliver 5 mA beams of deuteron up to 40 MeV and protons up to 35 MeV, CEA proposed a SARAF-LINAC reference design made of:

- an optional 4-vane RFQ bunching and accelerating 5 mA-cw beams from 20 keV/u to 1.3 MeV/u,
- a MEBT measuring, cleaning and matching the beam to
- a superconducting linac accelerating the beams to 40 MeV deuteron or 35 MeV proton,
- and the associated local control systems.

This design is based on beam dynamics calculations made with TraceWIN codes package developed at CEA [2] where the beam is represented by about 1M macro-particles.

## RFQ SIMULATIONS

The initial beam will be delivered by SARAF's source and LEBT built during phase 1. Measurements 1.4 m upstream the RFQ exhibit that the beam RMS normalized emittance is around (and even below)  $0.2 \pi \cdot \text{mm} \cdot \text{mrad}$  [3]. Therefore, we considered as simulation input deuteron and proton beams of  $0.2 \pi \cdot \text{mm} \cdot \text{mrad}$  rms emittance with a Gaussian distribution truncated to  $\pm 4$  sigmas (Fig.1). In the reference design [1], the 3.85 m long, 4-vane RFQ proposed by CEA is considered. It has:

- a constant 4 mm average radius R0, except at entrance and exit where it is increased to 6 mm in a few cells to reduce the input/output beam con/divergence.
- a constant voltage limited to 70 kV corresponding to a peak field of 1.6 Kp,
- a maximum sine vane modulation of 2.

The input energy is 20 keV/u and the output energy is 1.3 MeV/u. The matched beams density profiles are plotted on Fig. 2. The exit beam phase-space distribution of deuteron beam is plotted in Fig. 3. Please note that all the densities plotted in this paper are in logarithm scale.

Good transmission, low longitudinal emittance (Table 1) and no transverse emittance growth are observed.

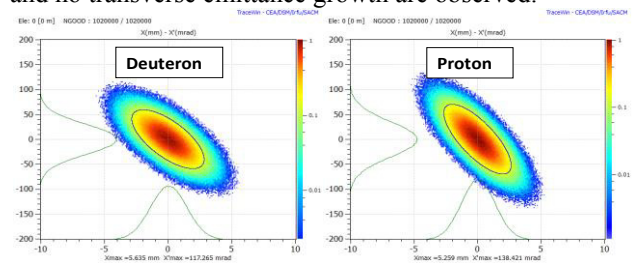


Figure 1: Input beam  $(x,x')$  distributions (matched to RFQ).

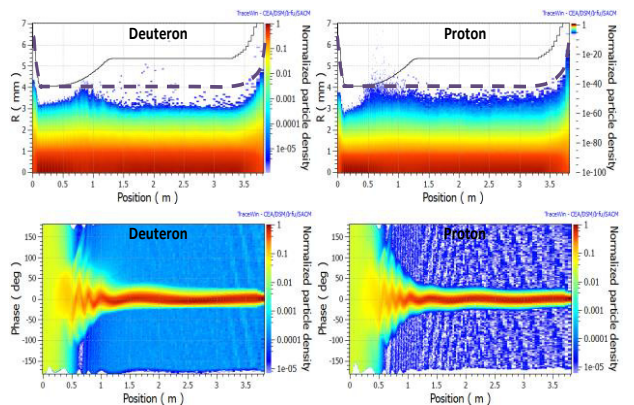


Figure 2: Matched beam density profiles in the RFQ.

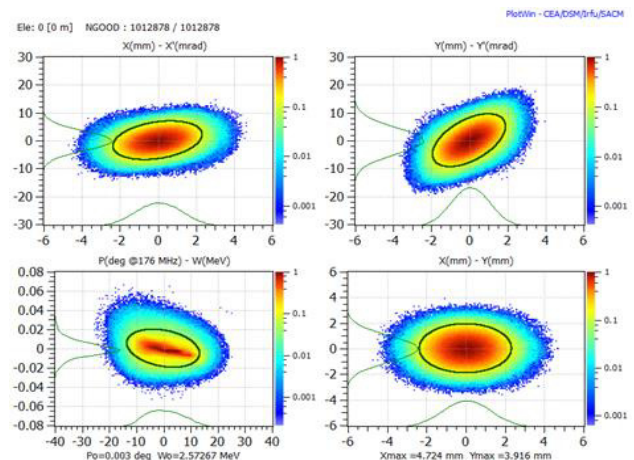


Figure 3: Deuteron beam phase-space distributions at RFQ exit.

Table 1: RFQ Performances

Particle	Transmission	Long. Rms emittance $\pi \cdot \text{mm} \cdot \text{mrad} (\pi \cdot \text{keV/u})$
Deuteron	99.3% (70 kV)	0.161 (31.8)
Proton	99.9% (50 kV)	0.194 (38.4)

## MEBT SIMULATION

The 4.7 m MEBT roles and main components are given in [1]. Room is left for a LINAC4/SPIRAL2-like fast chopper system expecting to switch 1kV in less than 4.5 ns. A 100% separation efficiency is obtained (for deuterons) with 800 V (Fig. 4).

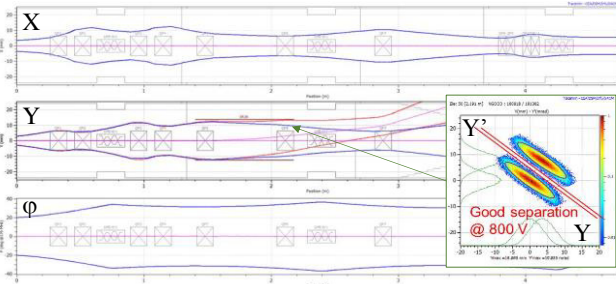


Figure 4: Beam  $\pm 3$  sigmas envelopes with (red) and without (blue) 800 V deflection voltage.

Three pairs of slits have been putted in the MEBT in order to suppress possible halo exiting from the RFQ (even if RFQ is also a good scraper itself). The phase-space area which will be selected by these slits can be seen at the exit of the RFQ and superimposed to the beam distribution at this position (Fig. 5). The slit system allows a good shaping of the beam in the transverse phase-space. The slits apertures are tuned to intercept about 0.1% of the beam per jaw.

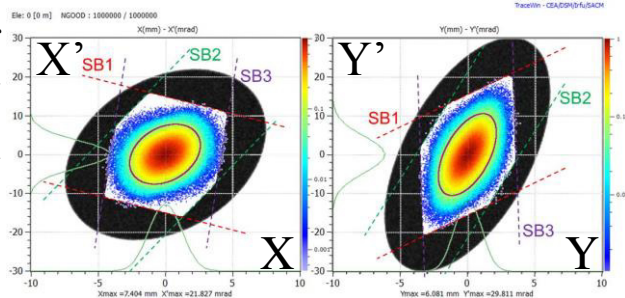


Figure 5: Slit system phase-space shaping seen from RFQ exit.

## SCL SIMULATION

The 20 m SCL is made of 2 identical 4.6 m cryomodules (CM1&2) housing 6 low-beta HWR cavities and 6 solenoid packages and of 2 identical 5.0 m cryomodules (CM3&4) housing 7 high-beta HWR cavities and 4 solenoid packages [1] (Fig. 6).

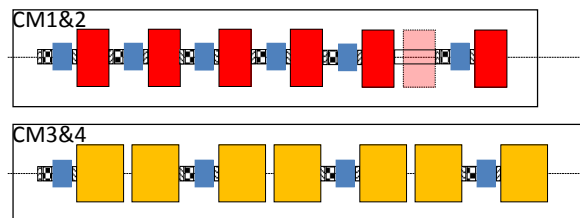


Figure 6: Cryomodule simplified schemes.

- The cavity field/phase and solenoid fields are tuned to:
- keep the longitudinal and transverse envelopes as regular as possible (match the beam),
  - with an accelerating field below 6.5 MV/m and 7.5 MV/m in respectively low- and high-beta cavities, to keep the peak magnetic and electric fields below 58 mT and 35 MV/m,
  - with a synchronous phase in each cavity chosen to keep a bucket large enough to limit particle unhooked,
  - with an on-axis magnetic field below 5.8 T.

The beam associated density profile (in log. scale) in both MEBT and SCL are plotted on Fig. 7, exhibiting good margins with respect to the pipe in the SCL.

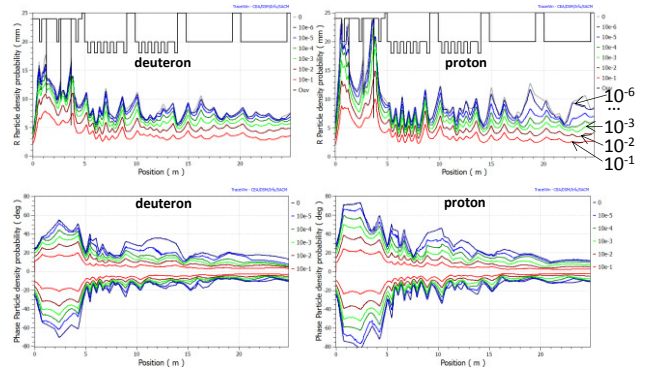


Figure 7: Deuteron (left) and proton (right) beam transverse (up) and longitudinal (down) logarithmic profiles.

## ERROR STUDIES AND BEAM LOSSES

Random errors have been applied to various linac elements (quadrupoles, solenoids, rebunchers and HWR cavities) of two types:

- Static errors are balanced by the diagnostics-correction scheme, based (here) on coupling between BPM and steerers in MEBT and SCL;
- Dynamic errors whose effect are not corrected.

The applied errors are given in Table 2 and Table 3.  $\pm 250\mu\text{m}$  BPM measurement errors have been assumed

Table 2: Error Amplitudes in MEBT on Quadrupoles (left) and Rebunchers (right)

Error type	Static	Dynamic	Error type	Static	Dynamic
$\Delta x$ [mm]	$\pm 0.2$	$\pm 0.010$	$\Delta x$ [mm]	$\pm 0.50$	$\pm 0.010$
$\Delta y$ [mm]	$\pm 0.2$	$\pm 0.010$	$\Delta y$ [mm]	$\pm 0.50$	$\pm 0.010$
$\theta_x$ [°]	$\pm 0.1$	$\pm 0.005$	$\theta_x$ [°]	$\pm 0.12$	$\pm 0.005$
$\theta_y$ [°]	$\pm 0.1$	$\pm 0.005$	$\theta_y$ [°]	$\pm 0.12$	$\pm 0.005$
$\theta_z$ [°]	$\pm 1$	$\pm 0.05$	$\Delta E/E$ [%]	$\pm 1$	$\pm 0.10$
$\Delta G/G$ [%]	$\pm 1$	$\pm 0.05$	$\phi$ [°]	$\pm 1$	$\pm 0.10$

Content from this work may be used under the terms of the CC BY 3.0 licence (© 2015). Any distribution of this work must maintain attribution to the author(s), title of the work, publisher, and DOI.

Table 3: Error Amplitudes in SCL on Solenoids (left) and HWR Cavities (right)

Error type	Static	Dynamic	Error type	Static	Dynamic
$\Delta x$ [mm]	$\pm 2$	$\pm 0.020$	$\Delta x$ [mm]	$\pm 2$	$\pm 0.02$
$\Delta y$ [mm]	$\pm 2$	$\pm 0.020$	$\Delta y$ [mm]	$\pm 2$	$\pm 0.02$
$\theta_x$ [°]	$\pm 0.8$	$\pm 0.008$	$\theta_x$ [°]	$\pm 0.8$	$\pm 0.01$
$\theta_y$ [°]	$\pm 0.8$	$\pm 0.008$	$\theta_y$ [°]	$\pm 0.8$	$\pm 0.01$
$\theta_z$ [°]	$\pm 1$	$\pm 0.10$	$\Delta E/E$ [%]	$\pm 1$	$\pm 0.1$
$\Delta G/G$ [%]	$\pm 1$	$\pm 0.05$	$\varphi$ [°]	$\pm 1$	$\pm 0.1$

Simulations of 1000 linacs with 500 000 macro-particles have been performed from RFQ input to SCL exit.

The resulting final extra emittance growth is plotted on Fig. 8. A +10% median emittance growth is obtained.

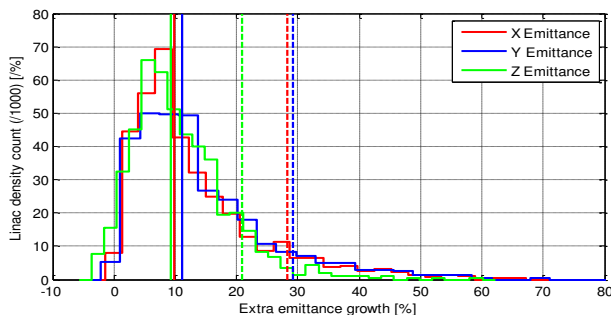


Figure 8 Final extra emittance growth distributions.

The transverse probability distribution of accelerated particles is plotted on Fig. 9. The longitudinal probability distribution is plotted on Fig. 10. It is clear that the particles losses are exclusively longitudinal, i.e. particles exiting the bucket.

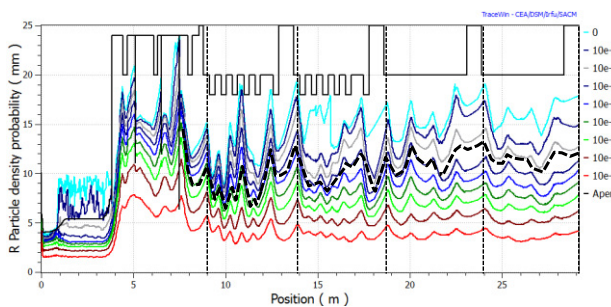


Figure 9: Radial probability distribution (over 8 decades). In dash black line, the acceptable level of losses per meter.

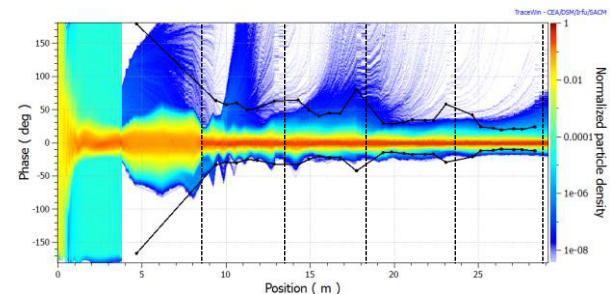


Figure 10: Longitudinal density probability (over 8 decades). Black lines exhibit the bucket phase limits.

In order to allow hands-on maintenance, level of beam losses much lower than 1 W/m are aimed:

- <150 nA/m under 5 MeV;
- <40 nA/m under 10 MeV;
- <5 nA/m under 20 MeV;
- <1 nA/m under 40 MeV.

These level correspond to acceptable losses.

When a macro-particle is lost (carrying statistically 5 mA/1000 linacs/500000 macro-particles = 0.01 nA), its smoothed contribution to the activation relative to the acceptable one can be plotted along the linac (Fig. 11). The losses are mostly in the focusing elements. They are 1% to 10% lower than the acceptable ones. Most of the activation is due to particles with energy lower than 10 MeV lost along the linac.

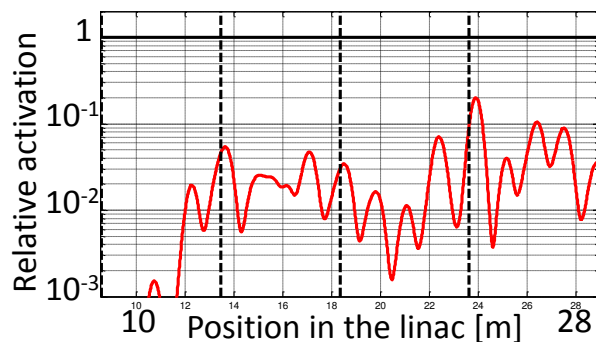


Figure 11: Estimated activation relative to hands-on acceptable level along linac.

## CONCLUSION

The beam dynamics studies of the SARAF-LINAC design have been done in nominal conditions and including errors on main components. Beam losses are caused by not-accelerated particles, finally hitting the beam pipe. In the reference design, the associated activation seems to be lower than the acceptable one allowing a hands-on maintenance. Nevertheless, in operating conditions, the number of not-accelerated particles can be controlled with the synchronous phase in the cavities to the expenses of a final energy change.

## REFERENCES

- [1] N. Pichoff et al., "The SARAF-LINAC Project for SARAF-Phase 2," THPF005, these proceedings, IPAC'15, Richmond VA, USA (2015).
- [2] N. Pichoff, P.A.P. Nghiem, D. Uriot, M. Valette, "Calculation of Halo in TraceWin code," IPAC'14, Dresden, Germany (2014).
- [3] L. Weissman et al. "SARAF Phase I linac in 2012," JINST 9 (2014) T05004, pp.1-29.